SPARSE ARRAYS FOR REAL-TIME 3D IMAGING, SIMULATED AND EXPERIMENTAL RESULTS

Andreas Austeng and Sverre Holm
Department of Informatics, University of Oslo, P.O.Box 1080 Blindern, N-0316 Oslo, Norway.

Abstract – This work presents the outputs from a project which aimed to lay the foundation of a 3D ultrasound imaging system where the emphasis was on real-time data acquisition and near real-time data visualization. To be able more precisely to describe the behavior of a sparse array system, a 25 Gbyte dataset containing every transmit and receive combination of a 50×50-element fully connected 3MHz array has been collected. The data have been processed off line on a cluster of 150 UNIX work stations to form experimental synthetic aperture 3D volume images.

We propose new methods based on the principle of suppression of grating lobes to form symmetric and non-symmetric regular sparse periodic and radially periodic designs. The performance of the new layouts come close to that of dense arrays. Our designs have simplicity in construction, flexibility in the number of active elements and possibility to trade off sidelobe peaks against sidelobe energy.

I INTRODUCTION

Two-dimensional phase steered arrays are proposed as the solution for real-time three-dimensional cardiac ultrasound imaging. Within the Esprit project "Real-Time 3D Ultrasound Imaging System with Advanced Transducer Arrays (NICE)", a 50×50 element 2D fully connected transducer array prototype has been produced [1]. The prototype, the NICE-array, is intended to demonstrate image quality and it is designed with a center frequency at 3 MHz and an element pitch equal to $.6\lambda$ (i.e. $308\mu m$). From this prototype, data from all transmit and receive combinations have been collected. By post-processing the data, we have formed experimental synthetic aperture 3D volume images for the dense and sparse designs.

One of the sparse array approaches which has gained most appreciation is sparse periodic layouts. These are based on the principle of having different transmit and receive layouts, where grating lobes in the transmit array response are suppressed by the receive array response and vice versa. The principle was applied to 2D arrays by Smith *et al.* [2]. In [3, 4], Vernier arrays were introduced. These arrays have good imaging performance and they are commonly used together with the dense array as a reference for array performance comparisons.

We propose new approaches for designing 2D layouts for 3D real-time imaging. The approaches include various periodic layouts with either symmetric or asymmetric periodicity, and periodicity either along the x and y axes, along the diagonals or along the radii. The simulations are based on a 48×48 element 2D array with center frequency and pitch similar to the NICE array. No apodization is considered for any of the layouts. All layouts have a circular footprint. This reduces the original 2304 elements by a factor of $\pi/4$ down to 1804 elements.

II MATERIALS AND METHODS

Our intention was to design layouts with performance better than a Vernier array. As a reference, we designed a Vernier $p = 3$ array, p being the sparseness factor. $p = 3$ is the smallest value of p which makes both the transmitter (Tx) and the receiver (Rx) sparse. The number of elements in the Vernier Tx and Rx was 421 and 208. We propose two new classes of sparse periodic designs.

Regular sparse periodic designs

To better suppress grating lobes, we propose to combine layouts with different symmetry axes, either between Tx and Rx or within a layout. Three examples are given.

Diag: Axial periodic Tx, diagonal periodic Rx.
As an improvement of a Vernier $p = 3$ Rx, we propose the layout with two elements on and then one off and so on, given in Figure 1(b). This layout has grating lobes as the reference Rx, but these are somewhat lowered. As Tx layout we propose the layout given in Figure 1(a). This layout has a non-sparse pattern along the diagonals, with an inter element spacing equal to

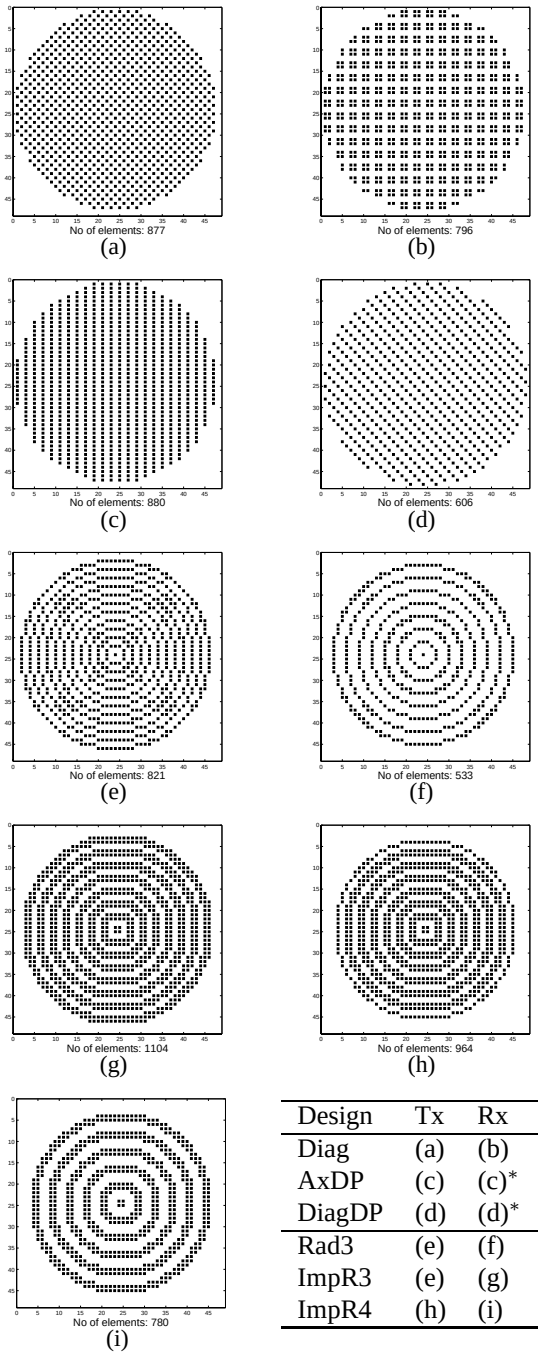

Design	Tx	Rx
Diag	(a)	(b)
AxDP	(c)	(c)*
DiagDP	(d)	(d)*
Rad3	(e)	(f)
ImpR3	(e)	(g)
ImpR4	(h)	(i)

Figure 1: Layouts.
The * indicates a 90° rotation.

$\sqrt{2}d$, d being the element pitch along the x or y axis. This layout is twice as dense as the reference Rx.

AxDP: Axial dense-periodic design.
The Tx layout of the second design is given in Figure 1(c). It has a periodicity of every second element along the x-axis, and is dense along the y-axis. The transmit layout will produce a response with grating lobes only along the axis corresponding to the x-axis of the layout. As Rx layout, the same pattern, but rotated 90°, is used.

DiagDP: Diagonal dense-periodic design.
The third design is constructed in the same way as the second, but the dense and sparse axes are along the diagonals instead of the x and y axis. The Tx layout is given in Figure 1(d), and the Rx layout is a 90° rotated version of the same layout.

Radially sparse periodic designs

As an alternative to regular sparse periodic layouts we propose radially sparse periodic layouts. These layouts are almost radially symmetric. This ensures a radiation pattern with no worst case direction. A layout is constructed by placing a 1D periodic array from the center and along an axis of the 2D array, and rotate it around the origin. Three examples are given.

Rad3: Radially periodic, p=3.
Radially periodic $p = 3$ layouts are designed by rotating 1D Vernier $p = 3$ arrays. The Tx layout is given in Figure 1(e) and the Rx layout is given in Figure 1(f).

ImpR3: Improved radially periodic, $p = 3$.
To improve a 1D Vernier $p = 3$ design, the Tx layout (every third element active) can be convolved with a kernel [1 1] to assure proper cancelation of the Rx grating lobe [5]. By rotating such an array one gets the Tx layout given in Figure 1(g). The Rx layout is the same as for the design *Rad3*.

ImpR4: Improved radially periodic, $p = 4$.
The improvement introduced in the design *ImpR3* can be used for both Tx and Rx. Starting with 1D Vernier $p = 4$ arrays, and convolve the Tx with a kernel [1 1] and the Rx with a kernel [1 0 1], one gets the Tx and Rx layouts as given in Figure 1(h) and 1(i).

Simulations

The pulse echo responses of each design were simulated using the program *FIELD II* [6]. The simulation parameters were speed of sound, $v = 1540$ m/s, center frequency, $f_0 = 3$ MHz, and sampling frequency, $f_s = 102$ MHz. The excitation was a one period sinusoid. Each element was simulated with a 66% -6dB beamwidth impulse response (a 3-period sinus with Hamming weighting). The focal range was 40 mm. For each response, the Integrated SideLobe Ratio (ISLR) defined as ratio between the energy in the mainlobe and the energy of the sidelobes in the radiation pattern, was calculated.

Design	BW			ISLR	PEAK
	-6dB	-20dB	-50dB	-50dB	">.2"
Dense	2.03	3.81	10.82	-16.9	-69.6
Vern	2.05	3.83	10.65	-3.8	-39.9
Diag	2.05	3.84	11.09	-13.3	-60.0
AxDP	2.05	3.85	11.21	-14.4	-62.5
DiagDP	2.02	3.79	10.65	-12.2	-57.4
Rad3	2.13	4.00	11.63	-1.7	-63.4
ImpR3	2.12	3.97	11.72	-7.6	-63.7
ImpR4	2.23	4.14	12.17	-7.8	-64.9

Table 1: Results.
BW gives mainlobe beamwidth in degrees at different levels in the response. ISLR is defined from the -50dB BW, and PEAK gives the maximal peak in the sidelobe region in the response for "$\sin\theta > .2$".

Experimental data

The experimental data was collected with a GE Vingmed Ultrasound scanner with 20 MHz sampling frequency and 12 bits AD-converter. The excitation used was a one period sinusoid. The prototype was designed such that 100 Tx elements and 100 Rx elements could be connected to the scanner at the same time. To collect all combinations, manual switching of one hundred elements had to be performed 625 times. The received signal was pre-amplified before digitization. The phantom imaged consisted of several nylon wires and one copper wire. The data was up-sampled with a factor of four, bandpass filtered and beamformed to volume images. The beamformer algorithm compensated for the temperature variations which had occurred during the recording of the data. Dynamic focusing was used for both transmit and receive. The total processing time to beamform a $60^\circ \times 60^\circ$ pyramid consisting of 3600 beams and with 10 cm depth for the dense design, the Vernier design and the six proposed designs was approximately 5000 CPU-hours on machines comparable to a Sun ULTRA1.

III Results

To simplify the comparison of different responses, the worst-case cut for each response is plotted in Figure 2. The worst-case cut is defined as the maximal value of the response for incident beams having an angle ϕ to the z axis which goes from the center and outwards, perpendicular to the array. Table 1 summarizes the figures calculated for the different layouts.

Figure 3 shows cuts in the experimental volume image of the elevation and azimuth plane broadside of the array for the design *AxDP*. The image is shown with 60 dB dynamic range. Figure 4 shows a cut of the copper-wire in the azimuth plane shown in Figure 3 for all designs. The wire is situated at approximately 4.2 cm depth and goes perpendicular to the azimuth direction.

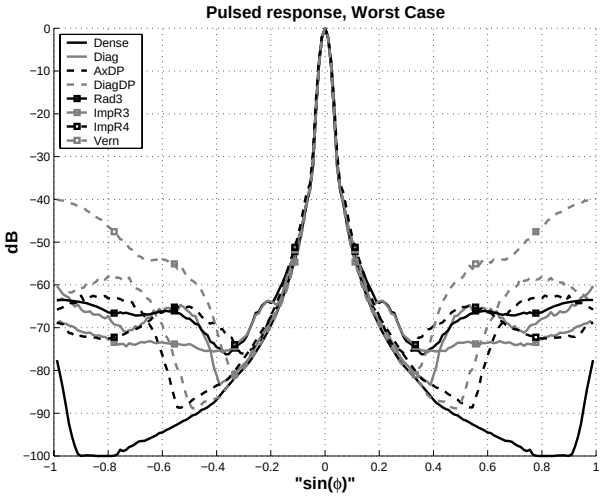

Figure 2: Simulated results.

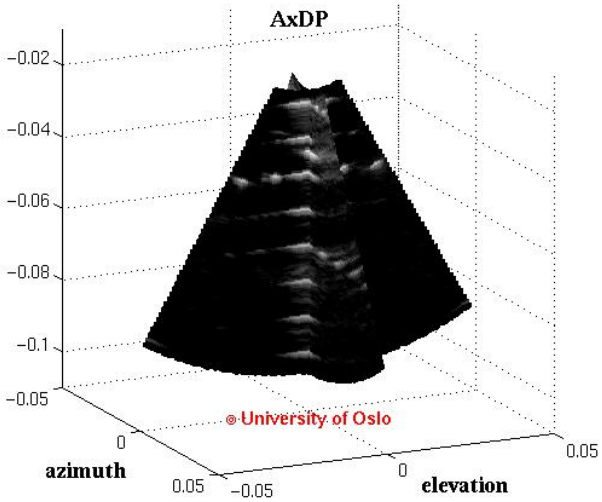

Figure 3: Volumetric data for design *AxDP*.

IV Discussion

The data set seems to be of acceptable quality and shows that the probe and data acquisition system meet our expectations. The worst case cut of the simulated pulse responses in Figure 2 shows that the sparse arrays proposed here outperform the Vernier layout with 10–

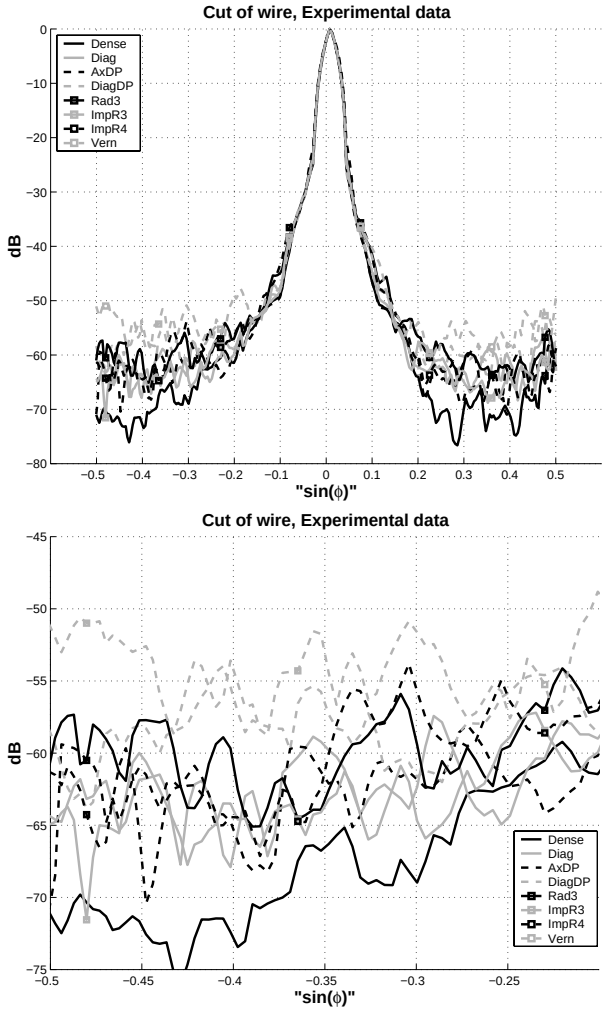

Figure 4: Cut of copper wire, full and zoomed.

20 dB.

The experimental results, summarized in Figure 4, show much of the same trend even if the differences between the different layouts are not as significant. However, in general the best arrays in the simulation are also the best arrays in the experiment.

Possible reasons for the discrepancy between the simulated and experimental responses can be minor variations in the speed of sound. Although compensated for, there could still be some fluctuation left. This will appear as a small, random delay error that will increase the sidelobe level. Some random sidelobe variation could also be caused by variation in sensitivity of each element.

The new sparse array designs presented here can be grouped in three categories according to the sum of the Rx and Tx channels that are required. Category A includes the Vernier sparse array (629 channels, overlap 48). Category B includes the DiagDP (1212, 208) and Rad3 layouts (1354, 221), and Category C contains the Diag array (1673, 396), AxDp (1760, 428), ImpR3 (1925, 551) and ImpR4 (1744, 484).

Imaging performance from the experiment follows these categories and correlates with the simulations although there is less difference in the experiment than in the simulations.

The arrays in categories B and C demonstrate that one can obtain much better results than the Vernier array. These arrays, especially those of Category C, approach an image quality which is quite close to that of the dense array.

V Acknowledgement

This work was partly sponsored by the Norwegian Research Council (NFR) under contract 11 6831/320 and by the ESPRIT program of the European Union under contract EP 22982. We also thank J. O. Erstad of GE Vingmed Ultrasound and J.-M. Bureau of Thomson Microsonics for collaboration during the experiments.

References

[1] J.-M. Bureau, W. Steichen, and G. Lepail. A two-dimensional transducer array for real-time 3D medical ultrasound imaging. In *Proc. IEEE Ultrason. Symp.*, pp 1065–1068, Japan, 1998.

[2] S. W. Smith, H. G. Pavy, and O. T. von Ramm. High-speed ultrasound volumetric imaging system. Part I: Transducer design and beam steering. *IEEE Trans. Ultrason., Ferroelect., Freq. Contr.*, 38(2):100–108, 1991.

[3] G. R. Lockwood, P.-C. Li, M. O'Donnell, and F. S. Foster. Optimizing the radiation pattern of sparse periodic linear arrays. *IEEE Trans. Ultrason., Ferroelect., Freq. Contr.*, 43(1):7–14, Jan. 1996.

[4] G. R. Lockwood and F. S. Foster. Optimizing the radiation pattern of sparse periodic two-dimensional arrays. *IEEE Trans. Ultrason., Ferroelect., Freq. Contr.*, 43(1):15–19, Jan. 1996.

[5] A. Austeng and S. Holm. Simple weighting to enhance sparse periodic arrays. In *IEEE Int. Conf. Acoust., Speech, Sign. Proc.*, vol V, pp 3109–3112, June 2000.

[6] J. Jensen. Field: A program for simulating ultrasound systems. In *10th Nordic-Baltic Conference on Biomedical Imaging, Medical & Biological Engineering & Computing*, vol 34, Supp. 1, Part 1, pp 351–353, 1996.